Contact angle saturation in electrocapillary effect

ARTICLE · NOVEMBER 2005

READS
51

3 AUTHORS, INCLUDING:

Behrouz Abedian
Tufts University
45 PUBLICATIONS **345** CITATIONS

SEE PROFILE

Irreversible Electrowetting on Thin Fluoropolymer Films

Shaun Berry,*,† Jakub Kedzierski,† and Behrouz Abedian‡

MIT Lincoln Laboratory, 244 Wood St., Lexington, Massachusetts 02040, and Department of Mechanical Engineering, Tufts University, 204 Anderson Hall, 200 College Ave., Medford, Massachusetts 02155

Received June 14, 2007. In Final Form: September 17, 2007

A study was conducted to investigate electrowetting reversibility associated with repeated voltage actuations for an aqueous droplet situated on a silicon dioxide insulator coated with an amorphous fluoropolymer film ranging in thickness from 20 to 80 nm. The experimental results indicate that irreversible trapped charge may occur at the aqueous−solid interface, giving rise to contact angle relaxation. The accumulation of trapped charge was found to be related to the applied electric field intensity and the breakdown strength of the fluoropolymer. On the basis of the data, an empirical model was developed to estimate the amount of trapped charge in the fluoropolymer as well as the voltage threshold for the onset of irreversible electrowetting.

1. Introduction

Manipulating a liquid interface by the technique of electrowetting is attracting increasing research and development activities for microfluidic applications.[1] The electrowetting phenomenon is relatively simple to implement and when controlled correctly is a reversible process that is critical in many microfluidic applications. Areas where electrowetting is currently being developed include lab-on-a-chip systems,[2,3] variable focus lenses,[4,5] and electronic displays.[6] However, as attractive as electrowetting is, there are fundamental issues that still need to be understood in order for electrowetting to be realized in device applications. To date much of the fundamental research has focused on two main issues: reducing the voltage required to generate the electrowetting effect[7,8] and understanding the saturation phenomenon.[9−11] One area that has gone largely unexplored is the topic of reversibility associated with repeated electrowetting actuations.

In some microfluidic applications utilizing the electrowetting phenomenon, the devices may be a single-use item. In these types of systems, electrowetting repeatability associated with lifetime use may not be as much of a concern as other factors, such as cost. However, in applications where the system may experience thousands or even millions of electrowetting cycles during the device lifetime, as in a liquid lens or electronic display, reliability and physical aging due to irreversibility will be a major concern. To our knowledge, there are no published data with specific attention given to issues pertaining to electrowetting reversibility. Several authors mention issues of reliability associated with repeated electrowetting actuations; however, it was not the intended focus of their respective work.[8,12] Seyrat and Hayes[8] present some limited reliability results in their study on the characterization of amorphous fluoropolymer materials. In one experiment, 100 electrowetting switches from 0 to 200 V were performed on a thick fluoropolymer insulator (7 μm) with no observed deterioration in modulation. Another experiment using a thinner film (0.5 μm) was performed where they observed some deterioration in modulation and attributed it to a form of charging of the insulator.

The goal of the experimental work presented in this paper was to understand fundamental issues pertaining to electrowetting reversibility. In this study, no specific device application was considered; instead, the performance of various materials subjected to repeated voltage actuations was evaluated. Understanding the material performance and physical parameters that can cause premature aging due to irreversible actuation is ultimately critical to genuine microsize-fluidic devices utilizing electrowetting phenomenon.

2. Experimental Methods

The experimental setup is shown in Figure 1. The ground electrode and dielectric used (called the S-phase) was a phosphorus-doped Si wafer with a thermally grown oxide layer of thickness t_{ox}. An amorphous fluoropolymer (aFP) layer of thickness t_{aFP} was spun-on the oxide layer of an individual sample. After spinning, the sample was baked in air at 185 °C for 10 min. The S-phase was placed on a support stage and immersed in a quartz tank containing 99% purity dodecane (called the O-phase). An aqueous water droplet (referred to as W-phase) was placed on the aFP surface. The voltage was applied to a platinum (Pt) wire electrode that was in contact with the W-phase. Drop size was not controlled, but typically ranged from 1 to 2 mm in diameter.

During this study, several different water phases were investigated, including DI, 0.1 M NaCl solutions, and phases containing sodium dodecyl sulfate (SDS). In addition, two different fluoropolymers were evaluated: CYTOP (CTL-809M) from the Asahi Glass Co. and Teflon AF1600 from DuPont. The majority of testing was done with insulating layers consisting of CYTOP on oxide. The thickness of CYTOP investigated ranged from 20 to 80 nm and the thickness of the oxide investigated ranged from 10 to 100 nm.

Two types of electrowetting reversibility experiments were performed: 100% duty cycle and 75% duty cycle. During a 100% duty cycle test, voltage was applied and held constant, not cycled

* Corresponding author. E-mail: sberry@LL.mit.edu.
† MIT Lincoln Laboratory.
‡ Tufts University.

(1) Mugele, F.; Baret, J. C. *J. Phys.: Condens. Matter* **2005**, *17*, R705−R774.
(2) Hosono, H.; Satoh, W.; Fukuda, J.; Suzuki, H. *Sens. Actuators B* **2007**, *122* (2), 542−548.
(3) Srinvason, V.; Pamula, V.; Pollack, M.; Fair, R. *IEEE* **2003**, 327−330.
(4) Kuiper, S.; Hendriks, B. H. W. *Appl. Phys. Lett.* **2004**, *85* (7), 1128−1130.
(5) Berge, B.; Peseux, J. *Eur. Phys. J. E* **2000**, *3*, 159−163.
(6) Feenstra, B. J.; Hayes, R. A.; von Dijk, R.; Boom, R. G. H.; Wagemans, M. M. H.; Camps, I. G. J.; Giraldo, A.; vid. Heijden, B. IEEE: MEMS 2006, Instanbul, 2006.
(7) Moon, H.; Cho, S. K.; Garrell, R.; Kim, C. J. *J. Appl. Phys.* **2002**, *92* (7), 4080−4087.
(8) Seyrat, E.; Hayes, R. A. *J. Appl. Phys.* **2001**, *90* (3), 1383−1386.
(9) Verheijen, H. J. J.; Prins, M. W. J. *Langmuir* **1999**, *15*, 6616−6620.
(10) Vallet, M.; Vallade, M.; Berge, B. *Eur. Phys. J. B* **1999**, *11*, 583−591.
(11) Quinn, A.; Sedev, R.; Ralston, J. *J. Phys. Chem. B* **2005**, *109*, 6268−6275.
(12) Hayes, R.; Feenstra, B. J. *Nature* **2003**, *425*, 383−385.

10.1021/la7017743 CCC: $37.00
Published on Web 10/20/2007

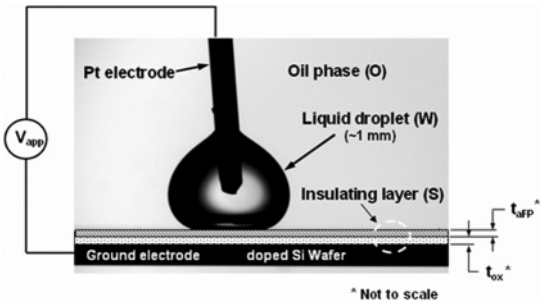

Figure 1. Experimental setup used in the electrowetting reversibility experiments.

on/off, throughout the duration of the test. In a 75% duty cycle test, the voltage was repeatedly cycled from a zero potential (voltage-off state) to an applied bias (voltage-on state). The voltage cycle period, applied as a step function, was 160 s total, 40 s off and 120 s on. The voltage on/off timing was controlled using the data acquisition software LABVIEW (National Instruments) and a ±10 V analog output board (NI PCI-6713). A voltage amplifier was used for test voltages > 10 V. In both types of reversibility tests, the contact angle at the three-phase interface was measured every 20 s using a Ramé-Hart goinometer (model 200) with the environmental fixture. A typical experiment was conducted over a period of several hours or even days. Both dc and ac biases were investigated and all sample preparation and experiments were conducted in a clean room environment.

An electrocapillary effect (ECE) curve was generated before and after the reversibility experiment using the same drop while maintaining the same location on sample. The ECE curve is the electrowetting contact angle profile curve obtained by incrementally increasing voltage. For a well-behaved system, the curve has a cosine-dependent profile that accurately follows electrowetting theory up to a saturation voltage.[1,13] Generating an ECE curve before and after the reversibility test allowed for verification of the integrity of the sample prior to starting an experiment, and served as a direct comparison of the quality of the ECE after the reversibility test. While generating the before ECE curve, the voltage was increased only until the test voltage to be applied in the reversibility experiment was reached. Our earlier work suggested that increasing the voltage to contact angle saturation was damaging to the insulating film.[13,14]

3. Results and Discussion

3.1. Results. Figure 2 shows results typically generated during an electrowetting reversibility experiment. The results are for a 75% duty cycle experiment for a W-phase of 1% SDS (wt %) in 0.1 M NaCl, an O-phase of dodecane ($\gamma_{wo} = 5.7$ mJ/m^2 is the surface energy between the W-phase and O-phase), and an S-phase of 83 nm CYTOP on 23 nm oxide cycled from 0 to −6 V dc. During this test, the drop experienced 649 voltage cycles, exposing the insulating layers to 19.2 h of accumulated voltage stress. Figure 2a shows the contact angle measurements collected during the voltage-on state. The data points in the figure represent the measurements made every 20 s. For clarity, the contact angle measurements collected during the voltage-off state are not shown. The zero-potential contact angle is ~160° for this water/oil/solid system. A solid line indicating the contact angle saturation point (electrowetting limit) for this system is included as a reference. Figure 2b shows the before and after ECE collected data. On the basis of the constant contact angle reached during each voltage cycle and overlapping before and after ECE curves, it can be argued that no electrowetting performance degradation occurred.

The majority of the reversibility experiments in this study were performed for a 24 h period. Subsequent to a number of

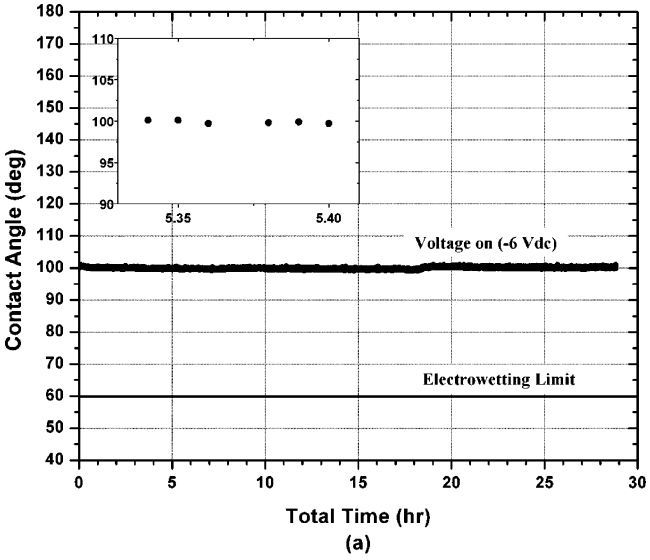

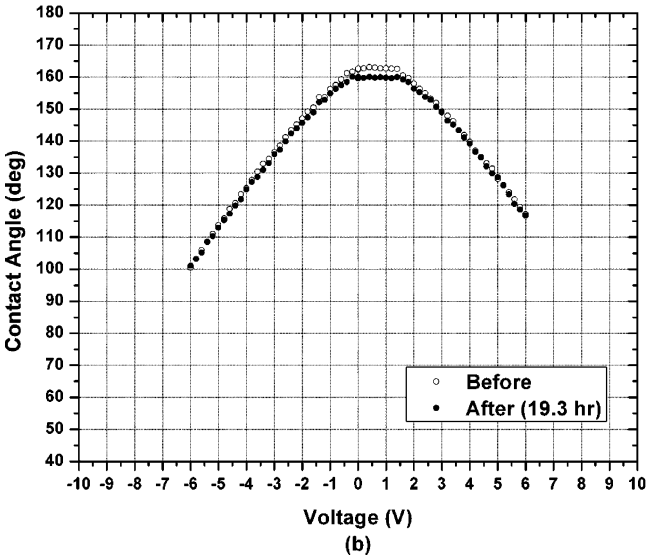

Figure 2. (a) Contact angle measurements from a 75% duty cycle experiment for a W-phase of 1% SDS in 0.1 M NaCl, an O-phase of dodecane ($\gamma_{wo} = 5.7$ mJ/m^2), and an S-phase of 83 nm CYTOP on 23 nm oxide cycled at −6 V dc; only contact angle measurements for the voltage on-state are shown. (Inset) Contact angle measurements during two voltage on-state cycles. (b) Before and after ECE curves. The drop experienced 649 voltage cycles, exposing the insulator layers to 19.2 h of voltage stress.

different initial experiments, it was observed that the time scale for physical or performance degradation to occur for this system was usually under 24 h. However, a few experiments were conducted for longer periods. The longest test conducted was a 75% duty cycle experiment for a W-phase of 0.1% SDS in 0.1 M NaCl, an O-phase of dodecane ($\gamma_{wo} = 6.1$ mJ/m^2), and an S-phase of 18 nm CYTOP on 30 nm oxide. In this test, the drop was actuated 3216 times from 0 to −3 V dc, exposing the dielectric layers to 107 h of accumulated voltage stress. During each voltage cycle the same contact angle was reach ($\theta = 110°$), i.e., no contact angle relaxation. As will be demonstrated, a change in contact angle per voltage cycle is an indication that some type of physical degradation of the system has occurred. The result from this experiment is encouraging, since it demonstrated that an insulator consisting of an extremely thin dielectric stack, <50 nm ($t_{aFP} = 18$ nm and $t_{ox} = 30$ nm), can be used in reversible electrowetting devices requiring numerous modulations.

(13) Berry, S.; Kedzierski, J.; Abedian, B. *J. Colloid Interface Sci.* **2006**, *303*, 517−524.
(14) Kedzierski, J.; Berry, S. *Langmuir* **2006**, *22*, 5690−5696.

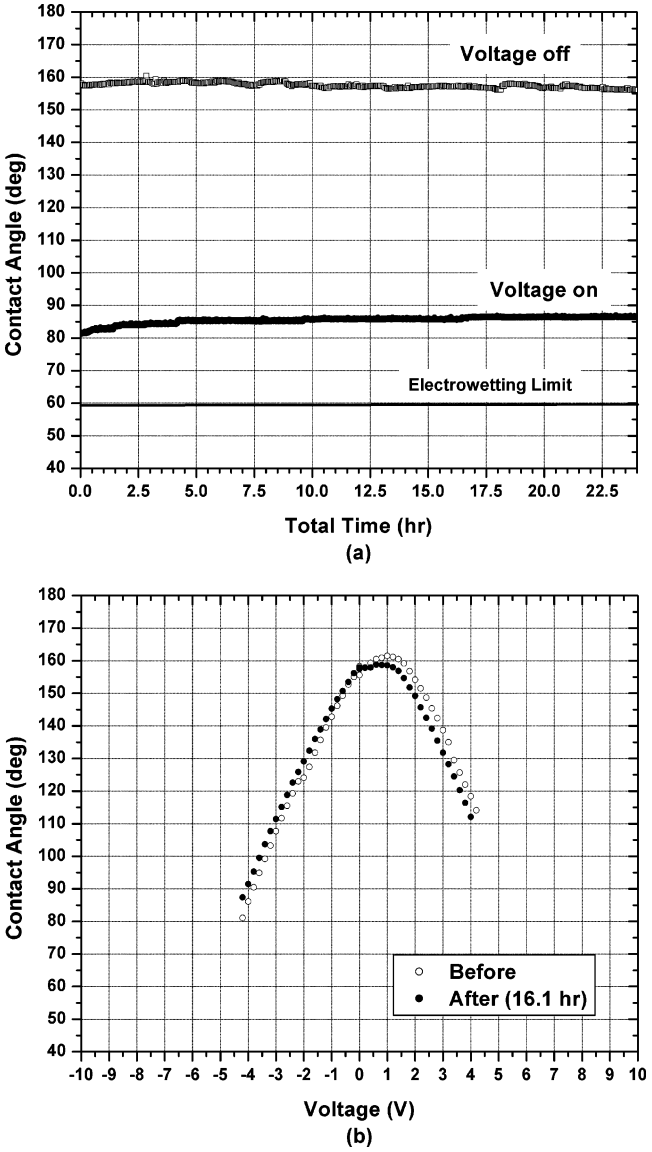

Figure 3. (a) Contact angles measurements from a 75% duty cycle experiment for a W-phase of 1% SDS in 0.1 M NaCl, an O-phase of dodecane ($\gamma_{wo} = 5.7$ mJ/m^2), and an S-phase of 16 nm CYTOP on 30 nm oxide cycled at −4.2 V dc. (b) Before and after ECE curves, note the shift in curves. The drop experienced 544 voltage cycles for a total 16.1 h.

Not all reversibility experiments resulted in clean electrowetting behavior throughout the duration of the test. Under certain conditions, the contact angle reached for the same applied voltage began to change with time. Figure 3 shows the results from a 75% duty cycle experiment for a W-phase of 1% SDS (wt %) in 0.1 M NaCl, an O-phase of dodecane, and an S-phase of 16 nm CYTOP on 30 nm oxide cycled from 0 to −4.2 V dc. In this experiment, the drop was cycled 544 times for a total of 16.1 h of voltage exposure to the insulator. The result shows that the contact angle reached during each voltage cycle was relaxing, meaning the drop was not wetting as far for the same voltage. During the test, the contact angle changed approximately 10° during the voltage-on state. In addition, there was a fundamental shift between the before and after ECE curves, as shown in Figure 3b. One explanation for the shift in the ECE curves, as well as with the change in contact angle with time, is that the surface of the fluoropolymer has trapped charge.

3.2. Charge Trapping. In normal electrowetting actuation, when a potential is applied to the drop surface, charge forms at the liquid/solid interface. This interfacial charging changes the free energy at the liquid/solid interface, causing the drop to spread as it seeks a new equilibrium state. When the potential is removed, the surface charge should completely dissipate, returning the droplet to its zero-potential state. This is the essence of a reversible electrowetting effect. Under certain conditions, however, it is possible for the charged species to become trapped in fluoropolymer and remain after the potential is removed. In the case of the reversibility test result presented in Figure 3, contact angle relaxation per voltage cycle is taken as an indication that the surface of the fluoropolymer accumulated a trapped charge that affected the electrowetting performance. The accumulation of trapped charge can cause several visible effects during an experiment. The wetted contact angle changes with repeated voltage cycles and/or the drop behaves erratically during the electrowetting process. In some extreme cases, the droplet no longer responds to changes in applied voltage.

The trapped charge phenomenon has also been observed and proposed as a concern by other researchers[8,9,15] and is often thought to be one of the conditions associated with contact angle saturation.[8,9] Verheijen and Prins[9] offer some detailed discussion about charge trapping on an aFP surface and present a charge model based on first principles. In their analysis, they assume ions in the liquid become trapped in fluoropolymer due to electrostatic forces and form a uniform charge distribution that they argue causes a reduction in the electrowetting force. This is consistent with our own experimental data in which a relaxation in contact angle was seen when charge trapping is believed to have occurred.

Even though other researchers have observed this charging phenomenon, little has been done quantitatively to describe the conditions for which it manifests in electrowetting systems. After reviewing all the data collected during this study, the following correlation was observed: irreversible charging of the solid phase is coupled with the electric field intensity and the dielectric strength of the aFP layer. The argument is that trapped charge accumulates on or in the aFP layer when the electric field intensity exceeds the effective dielectric strength of the aFP material. It should be noted that exceeding the effective dielectric strength of the aFP layer does not cause complete dielectric breakdown of the insulator stack nor is it necessarily a condition for contact angle saturation. From our previous experimental work,[13] complete dielectric breakdown occurred when the field intensity exceeded the higher strength dielectric in the insulator stack, which in our systems is oxide. In the same study, it was also shown that contact angle saturation is not a field effect and that the electrowetting process can continue even when the dielectric strength of the aFP layer is exceeded.[13] It is also important to remember that charge trapping occurs during contact angle saturation, which is not dependent on the field. Saturation-induced charging is not addressed in this work.

Since the argument is that charge trapping occurs when the effective dielectric strength of the aFP layer is exceeded, a voltage threshold, V_T, is defined as the voltage applied that causes the electric field intensity across the fluoropolymer, E_{aFP}, to equal the effective dielectric strength, D_{aFP}. The threshold voltage is given by

$$V_T = D_{aFP}\left(t_{aFP} + \frac{\epsilon_{aFP}}{\epsilon_{ox}} t_{ox}\right) \quad (1)$$

where ϵ_{aFP} is the dielectric constant of the aFP, ϵ_{ox} is the dielectric constant of the oxide, and t_{aFP} and t_{ox} are the thicknesses of the

(15) Janocha, B.; Bauser, H.; Oehr, C.; Brunner, H.; Göpel, W. *Langmuir* **2000**, *16*, 3349−3354.

Table 1. Electrical Properties

	dielectric constant (ϵ)	dielectric strength (V/nm)
CYTOP	2.1	0.110
AF1600	1.93	0.021
SiO_2	3.9	0.1−1.0

aFP and oxide layers, respectively. Table 1 shows the electrical properties of CYTOP,[16] Teflon AF1600,[17] and SiO_2. If $|V_{app}| > V_T$, where V_{app} is the applied test potential, it is expected that contact angle relaxation will eventually result due to charge trapping, and if $|V_{app}| < V_T$, no electrowetting performance decay is anticipated in the form of trapped charge.

The threshold voltage for the system shown in Figure 2 (83 nm CYTOP on 23 nm oxide) is $V_T = 10.5$ V. The applied voltage for this test was $|V_{app}| = 6$ V dc, which is lower than V_T, and as a result indicates there was no contact angle relaxation or asymmetric wetting behavior. This result is in contrast with the result shown in Figure 3. For this system (16 nm CYTOP on 30 nm oxide) the threshold voltage is $V_T = 3.5$ V. The test voltage was $|V_{app}| = 4.2$ V dc, and as the result shows, there was a change in contact angle with time, as well as a shift between the before and after ECE curves.

The correlation with the dielectric strength of the aFP layer and charge trapping was independent of the different water phases tested, the different thicknesses of the insulator layers tested, and the different applied potentials, including voltage polarity. Figure 4 shows contact angle values collected during the voltage-on state from three different 75% duty cycle reversibility experiments for a W-phase of 0.1 M NaCl, an O-phase of dodecane ($\gamma_{wo} = 56$ mJ/m^2), and an S-phase of 92 nm CYTOP on 30 nm oxide. For this insulator system, the threshold voltage is $V_T = 11.9$ V. As the figure shows, the only test result that showed no contact angle relaxation with voltage cycle was the test conducted at $|V_{app}| = 10$ V dc, which is below the threshold voltage. In the experiments where the applied voltage value exceeded V_T, changes in contact angle with voltage cycle were observed. Thus, the reversibility test results show no contact angle relaxation per voltage cycle if the applied voltage $|V_{app}| < V_T$, and when $|V_{app}| > V_T$, the test results indicate the surface over time traps charge, on the basis of the observed change in contact angle and erratic wetting behavior witnessed.

Figure 5 shows the amount of contact angle relaxation, $\Delta\theta$, after 1 h of voltage stress, plotted against the ratio of electric field intensity, E_{aFP}, divided by the effective dielectric strength of CYTOP, D_{aFP}. The data points in the figure are a collection of individual electrowetting reversibility tests for all the different water phases, different thickness of CYTOP and oxide, and different potentials used in this study. It is clear to see from the figure that when the ratio of $E_{aFP}/D_{aFP} > 1$, contact angle relaxation occurs, and for test conditions where $E_{aFP}/D_{aFP} < 1$, there is essentially no relaxation.

3.3. Trapped Charge Model. After reviewing the before and after ECE curves from experiments where charge trapping is suspected to have occurred, it can be argued that the trapped charge is uniformly distributed under the drop. For these experiments, there was a noticeable voltage shift between the before and after ECE profiles, as seen in Figure 3b. To review, ECE profiles are generated from the zero potential state. Voltage is increased incrementally with contact angle measurements made at each voltage increment (0.2 and 0.5 V were the voltage increments used in this study). When the drop is at its zero potential state, the initial contact angle is large, ~160° for this water/aFP/oil ambient system, and the drop contact area on the surface is small relative to the area the drop covers when at the test voltage used in reversibility experiment. If the trapped charge had a distinct spatial surface distribution, for example, localized only near the contact line of the drop when at the voltage-on state, then it would be expected that the after ECE profile be unaffected and follow the before ECE profile until the spread of the drop approached the wetting profile, i.e., the contact angle obtained during the reversibility test for the voltage-on state. The after ECE profiles from reversibility experiments where charge trapping occurred do not exhibit this behavior. There is deviation between the before and after profiles for all contact angles. In addition, the profile shapes are the same, only shifted, which indicates the surface energy between the drop and ambient phase has remained constant. However, it should be noted that

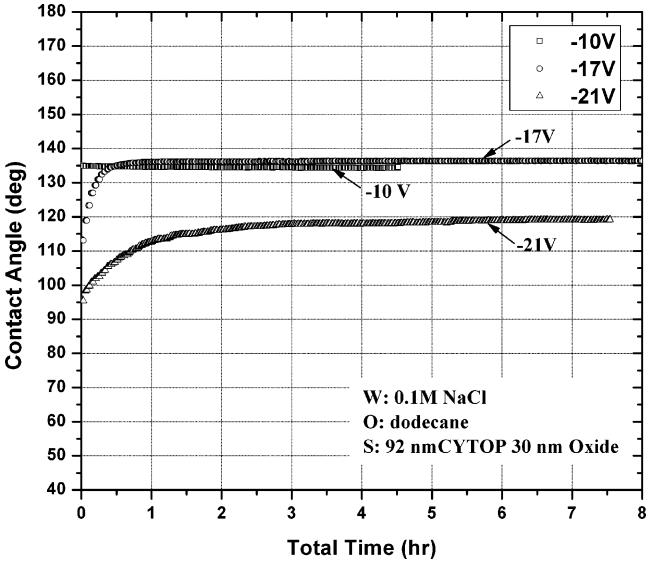

Figure 4. Contact angle measurements during the voltage-on state from 75% duty cycle experiments for a W-phase of 0.1 M NaCl, an O-phase of dodecane ($\gamma_{wo} = 56$ mJ/m^2), and an S-phase of 92 nm CYTOP on 30 nm oxide. The threshold voltage for this system is estimated at $V_T = 11.9$ V.

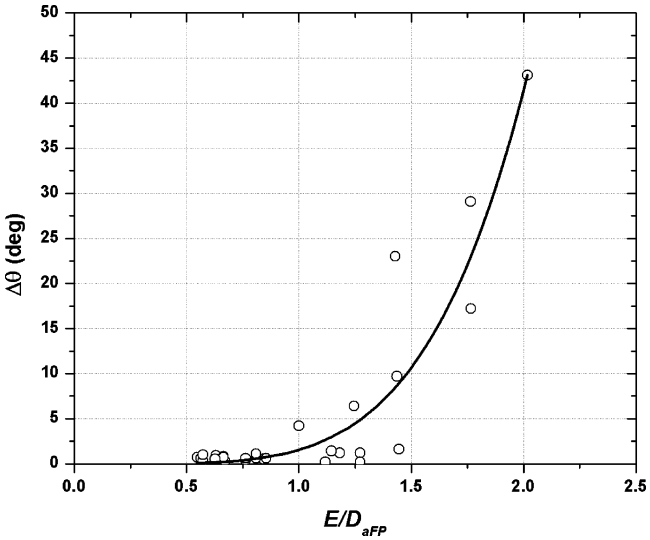

Figure 5. Summary of reliability test data plotting the change in contact angle observed after 1 h of testing vs the nondimensionalized electric field intensity across the aFP. D_{aFP} is the effective dielectric strength of the aFP material. Data points represent individual experiments. Solid line represents a least-squares fit.

(16) Technical Bulletin, Bellex International Corp., Wilmington, DE.
(17) Teflon AF Product Information Bulletin, DuPont, Wilmington, DE.

for some after ECE curves the contact angle data is not as clean as the before profile, indicating some heterogeneity of the trapped charge probably exists, but overall it is predominately uniform.

Assuming a uniform charge distribution, the trapped charge density, σ_c, is defined by the following relationship

$$\sigma_c = CV_c \tag{2}$$

where C is the capacitance per unit area of the insulator stack and V_c is defined as the trapped charge potential. As the results show, when surface charge trapping occurred, it had the effect of lowering the electrowetting force, which was seen as a reduction in the contact angle with time. This behavior is consistent with the fundamental model derived by Verheijen and Prins.[9] Using this picture of the trapped charge tending to reduce the electrowetting force requires V_c to be a function of the change in contact angle and applied voltage.

Starting with the fundamental equation for electrowetting and accounting for a reduction in the electrowetting force resulting from charge trapping, the charge potential V_c is included in the quadratic term. The modified electrowetting equation accounting for charge trapping is

$$\cos\theta(V_{app}) = \cos\theta_0 + \frac{C[(V_{app} - V_{pzc}) - V_c]^2}{2\gamma_{wo}} \tag{3}$$

where $\theta(V_{app})$ is the contact angle as a function of applied voltage V_{app}, V_{pzc} is the voltage at the potential of zero charge (V_{pzc} is not necessarily equal to zero), θ_0 is the contact angle at the potential of zero charge, C is the capacitance of the dielectric per unit area, and γ_{wo} is the surface energy between the aqueous phase and the ambient phase. Equation 3 is the same expression reached by Verheijen and Prins[9] using a rigorous thermodynamic analysis. Here it was implicitly attained on the basis of experimental observations. When no charge trapping occurs, $V_c = 0$, and the fundamental equation of electrowetting is recovered.

Since V_c is defined as a function of the change in contact angle, an additional expression is required to determine its value. During the first voltage-on cycle, no trapped charge exists; thus, the fundamental equation of electrowetting can be used to predict the Lippmann contact angle. Subtracting the fundamental equation of electrowetting from eq 3 leads to

$$\frac{2\gamma_{wo}}{C}(\cos\theta_n - \cos\theta_1) = (V_{app} - V_{pzc} - V_c)^2 - (V_{app} - V_{pzc})^2 \tag{4}$$

where the subscripts n and 1 indicate the contact angle after n number of voltage cycles and the first voltage cycle, respectively. Rearranging eq 4 and solving for V_c give the equation

$$\frac{V_c}{V_{app} - V_{pzc}} = 1 - \left[\frac{2\gamma_{wo}}{C(V_{app} - V_{pzc})^2}(\cos\theta_n - \cos\theta_1) + 1\right]^{1/2} \tag{5}$$

Recognizing that $(V_{app} - V_{pzc})^2 = 2\gamma_{wo}/C(\cos\theta_1 - \cos\theta_0)$, where θ_0 is the contact angle at the potential of zero charge, the equation for V_c becomes

$$\frac{V_c}{V_{app} - V_{pzc}} = 1 - \left[\frac{\cos\theta_n - \cos\theta_1}{\cos\theta_1 - \cos\theta_0} + 1\right]^{1/2} \tag{6}$$

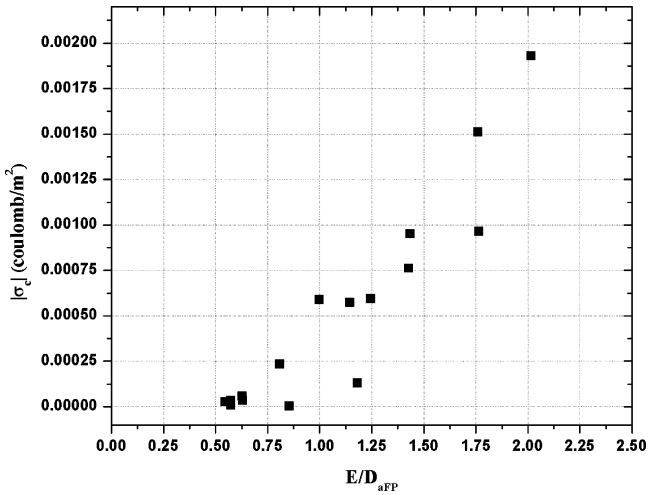

Figure 6. Plot the absolute value of trapped charge density, σ_c, vs the ratio of the electric field intensity divided by the effective dielectric strength of the aFP layer, E/D_{aFP}.

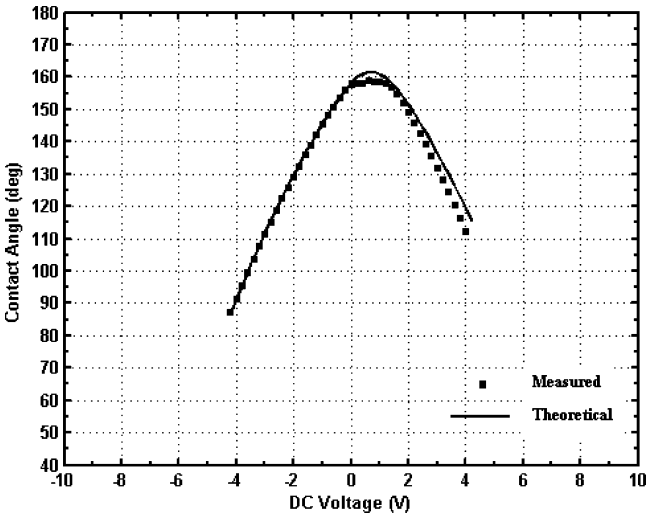

Figure 7. The after ECE profile from the 75% duty cycle experiment for a W-phase of 1% SDS in 0.1 M NaCl, an O-phase of dodecane, and an S-phase of 16 nm CYTOP on 30 nm oxide cycled at −4.2 V dc. Theoretical curve generated from the modified electrowetting equation for $V_c = -0.224$ V.

Using eq 6, a value for V_c can be determined. Once V_c is known, the trapped charge density can be estimated using eq 2. One interesting aspect of eq 6 is that it requires no knowledge of the material properties of the system, only knowing the contact angles. Figure 6 shows a plot of $|\sigma_c|$ vs the ratio E/D_{aFP} using data collected at the end of the reliability tests. As the plot shows, once the electric field intensity exceeds the effective dielectric strength, the amount of trapped charge grows linearly, at least over the range of E/D_{aFP} ratios tested in this study.

It was observed that, for small values of V_c, eq 3 can be used to predict the contact angle for any applied voltage. To illustrate this, contact angles using eq 3 for arbitrary voltages are compared with the after ECE profile shown in Figure 3b. Figure 7 plots the after ECE profile from the 75% duty cycle experiment shown in Figure 3 for a W-phase of 1% SDS (wt %) in 0.1 M NaCl, an O-phase of dodecane, and an S-phase of 16 nm CYTOP on 30 nm oxide cycled from 0 to −4.2 V dc, with the theoretical profile determined from eq 3. On the basis of eq 6, V_c for this test was found to be −0.224 V. As can be seen there is good agreement between the measured data and theoretical profile. Interestingly, for small values of V_c, the charge potential is

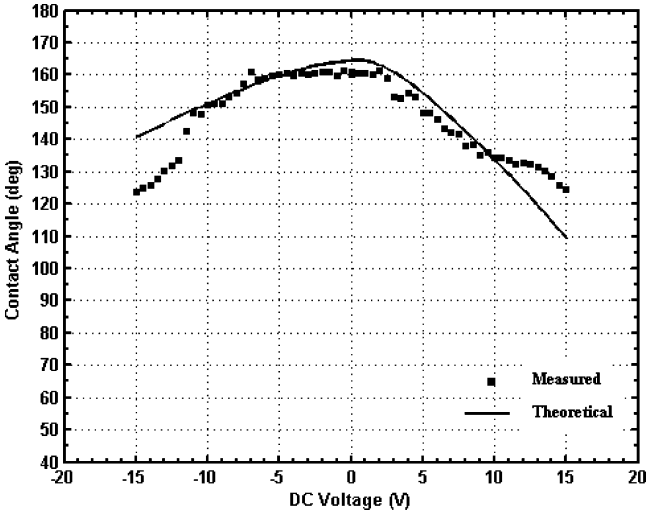

Figure 8. The after ECE profile from the 75% duty cycle experiment for a W-phase of 0.1 M NaCl, an O-phase of dodecane, and an S-phase of 83 nm CYTOP on 23 nm oxide cycled at −15 V dc. Theoretical curve generated from the modified electrowetting equation for $V_c = -4.89$ V.

equivalent to the amount of voltage shift seen between the before and after ECE curves. However, when the value of V_c is large, $\gg 1$, it was observed that the fit using eq 3 for arbitrary voltages with the after ECE curve is poor. In order to provide good agreement between eq 3 and the measured after ECE curve for this condition, an empirical parameter was needed.

It was found that an empirical parameter with a linear dependence on voltage provides excellent agreement. The general form of eq 3 that includes an empirical parameter for an arbitrary voltage value, V, and a known value of V_c becomes

$$\cos\theta(V) = \cos\theta_0 + \frac{C[(V - V_{pzc}) - \beta V_c]^2}{2\gamma_{wo}} \qquad (7)$$

where β is the empirical parameter defined as

$$\beta = \begin{bmatrix} 1 \text{ for } |V_c| < V_c^* \\ |V/V_{app}| \text{ for } |V_c| < V_c^* \end{bmatrix} \qquad (8)$$

where V_c^* is the critical charge potential. Thus, when $|V_c| < V_c^*$, β is equal to 1. In this range, V_c is essentially equal to the voltage shift between the before and after profiles, as seen in Figure 7. When $|V_c| > V_c^*$, β becomes a linear function of $|V/V_{app}|$, where V_{app} is the potential used to determine V_c from eq 6. For the system tested in this study, V_c^* was approximately 1. More experiments are needed to accurately determine this threshold, but based on comparing the after ECE curves collected during this study with profiles generated from eq 7, $V_c^* \cong 1$ appeared to be the critical value.

Figure 8 plots the after ECE profile from the 75% duty cycle experiment for a W-phase of 0.1 M NaCl, an O-phase of dodecane, and an S-phase of 83 nm CYTOP on 23 nm oxide cycled from 0 to −15 V dc, with the theoretical profile determined from eq 7. In this reversibility experiment, V_c was found to be −4.9 V, which is greater than V_c^*; thus, a linear dependency of β is used. As can be seen, using a linear dependency of β allowed for an accurate comparison between the measured data and calculated contact angles. A linear dependency of β on V in effect indicates that a change in capacitance C has occurred in these cases. A nonuniform spatial distribution of the trapped charge in the fluoropolymer could well cause a shift in C and explain the observed effect. In fact, on the basis of how well eq 7 fits the data, as well as the observed drop behavior during the after ECE measurements, a distinct spatial distribution of the trapped charge is probably forming at higher fields, i.e., large ratios of E/D_{aFP}. This distribution may be more concentrated out near the contact line the drop formed during the reversibility experiment. This observation is consistent with the fact that a nonuniform high electric field is experienced at the three-phase contact line, which has a zone of influence on the order of the dielectric thickness.[18] How this high field point contributes to the trapped charge is still open for debate. However, without direct measurement of the charge distribution, this is an indirect observation on our part. Equation 7 is presented with the caveat that the true trapped charge density distribution is not known and is assumed to be uniform.

3.4. CYTOP vs Teflon AF1600. The majority of the experiments conducted in this study were done with CYTOP as the hydrophobic material. However, a few reversibility experiments were conducted using Teflon AF1600. Teflon AF1600 is the fluoropolymer typically cited by other researchers working in the field of electrowetting;[3,4,7,8,19] thus, it was worth investigating its performance.

Several 75% duty cycle tests were performed for an S-phase of 23 nm AF1600 on 30 nm oxide, an O-phase of dodecane, and W-phases consisting of 0.1% SDS (wt %) in 0.1 M NaCl and 2% SDS (wt %) in 0.1 M NaCl. The voltage potential was cycled from 0 to −3 V dc for both water phases investigated. The results from these experiments suggest that the performance of AF1600 is poor at the film thickness of 23 nm on 30 nm oxide. The drop behavior became erratic within three voltage on/off cycles. The experiments had to be terminated within 10 min due to the excessive drop movement during actuation. In one experiment, the drop actually separated from the Pt. wire electrode. The poor performance of the AF1600 at this thickness is consistent with the work done by Seyrat and Hayes.[8] In their study, they claim that for coating thicknesses <400 nm (0.4 μm) the electrical properties and thus performance of AF1600 deteriorate dramatically. The results are also consistent with the charge trapping model, where erratic behavior manifests when the electric field intensity exceeds the effective dielectric strength of the fluoropolymer. On the basis of the properties listed in Table 1, the threshold voltage for this S-phase was $V_T = 0.8$ V, and the applied potential was 3 V dc, resulting in a high ratio of $E/D_{aFP} = 3.75$.

To investigate the AF1600 behavior more thoroughly, thicker insulators were tested. This allowed lower electric field intensities while still generating reasonable electrowetting modulation. Figure 9 shows the result from a 75% duty cycle test for a W-phase of 0.03% SDS (wt %) in 0.1 M NaCl, an O-phase of dodecane ($\gamma_{wo} = 7.7$ mJ/m^2), and an S-phase of 85 nm AF1600 on 30 nm oxide cycled from 0 to −3 V dc. In this experiment, the drop was cycled 182 times, exposing the insulator layers to 5.4 h of accumulated voltage stress. The threshold voltage for this test was $V_T = 2.1$ V, which was less than the test voltage. As Figure 9a indicates, there was a change in contact angle with voltage cycle, consistent with the model. However, unlike the gradual contact angle relaxation observed with CYTOP when $|V_{app}| > V_T$, there was a sudden jump in the contact angle with AF1600. Using eqs 6 and 2, V_c and σ_c were determined to be −1.475 V and -2.52×10^{-4} C/m^2, respectively.

(18) Mugele, F.; Buehrle, J. *J. Phys.: Condens. Matter* **2007**, *19*, 1−20.
(19) Millefiorini, S.; Tkaczyk, A.; Sedev, R.; Efthimiadis, J.; Ralston, J. *J. Am. Chem. Soc.* **2006**, *128*, 3098−3101.

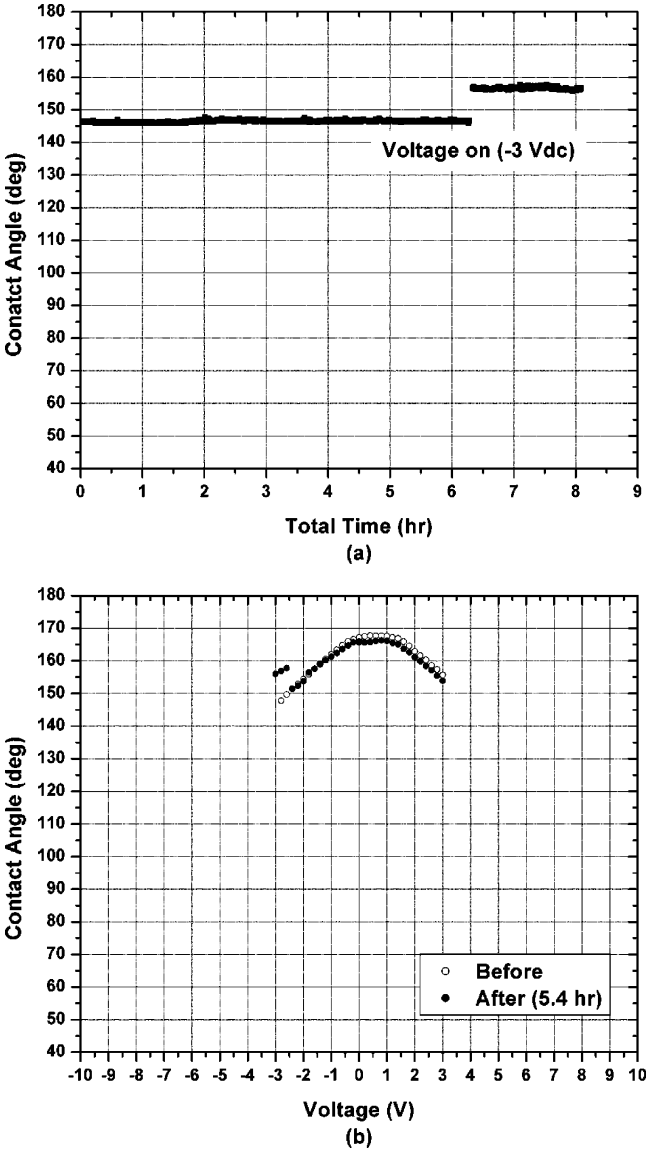

Figure 9. Reliability results from 75% duty cycle test for a W-phase of 0.03% SDS in 0.1 M NaCl, an O-phase of dodecane ($\gamma_{wo} = 7.7$ mJ/m^2), and an S-phase of 85 nm AF1600 on 30 nm oxide cycled from 0 to −3 V dc. The drop cycled 182 times, exposing the dielectric layers to 5.4 h of accumulated voltage stress. (a) Contact angle vs time. (b) Before and after ECE curves.

Additional tests were done using 71 nm AF1600 on 940 nm oxide. This allowed for experiments to be conducted above and below V_T. The threshold voltage for this S-phase was calculated at $V_T = 11.3$ V. Two 75% duty cycle reversibility tests were performed, one at −9.5 V dc, below V_T, and one at −16 V dc, above V_T. The same system was used for both test voltages, which consisted of a W-phase of 0.03% SDS (wt %) in 0.1 M NaCl, an O-phase of dodecane, and an S-phase of 71 nm AF1600 on 940 nm oxide. The result from $V_{app} = -9.5$ V dc showed no change in contact angle versus voltage cycle, indicating no performance degradation over this test period. In this test, the drop was cycled 467 times, exposing the insulator to 13.8 h of voltage stress. In the $V_{app} = -16$ V dc test, there was no change in contact angle for the first 15 h. However, after 15 h of testing, there was a sudden jump in contact angle. Once the jump occurred, electrowetting behavior became erratic and the test was terminated, since the drop was about to separate from the electrode. The before and after ECE curves (not shown) from this test do show a fundamental shift between the two curves. This is consistent with the behavior seen with CYTOP when charge trapping is believed to have occurred. Also consistent with the result shown in Figure 9 was the sudden change in contact angle, which were unlike experiments with CYTOP, where contact angle relaxation was more gradual over time.

4. Summary

The goal of this experimental effort was to understand parameters that effect electrowetting reversibility for aqueous water systems consisting of insulators with oxide and an amorphous fluoropolymer. The experimental data indicates the most dominate form of electrowetting performance decay for the system tested was the accumulation of trapped charge, which was found to be related to the electric field intensity exceeding the effective dielectric strength of the fluoropolymer. This correlation was independent of the different water phases tested, the thicknesses of oxide and fluoropolymer, and the polarity of the applied potential. It should be noted that this correlation is for this type of liquid/solid system. Other liquid/solid phases used for electrowetting may have more dominant forms of performance decay other than charge trapping or display the signs of irreversible charging differently than what was observed in this study. In our previous work with alcohol-based surfactants added to the water phase, the time scale for decay was so rapid that it was clear other thermodynamic or surface kinetic conditions were the issue.[14]

The condition when the electric field intensity is equal to the effective dielectric strength was correlated to a threshold voltage term. The voltage threshold term can be used to predict if a test voltage will be damaging to the fluoropolymer. In experiments where the test voltage was greater than the threshold voltage, electrowetting performance decreased over time and was seen as a reduction in the electrowetting force. The reduction in electrowetting force is believed to be caused by a charge becoming trapped in or on the fluoropolymer. In this study, no direct method was used to quantify the magnitude of the charge or its spatial distribution; however, the experimental data indicates that the trapped charge has a uniform distribution under the drop for values of $V_c < V^*$ and possibly has a nonuniform spatial distribution for values of $V_c > V^*$.

Finally, a performance comparison was made between CYTOP and AF1600. For the thicknesses used in this study, CYTOP has superior electrowetting reversibility. This performance difference is attributed to the higher effective dielectric strength.

Acknowledgment. This work was sponsored by the United States Air Force under contract #FA8721-05-C-002. Opinions, interpretations, conclusions, and recommendations are those of the author and are not necessarily endorsed by the United States Government.

LA7017743